Mathematical model for the power supply system of an autonomous object with an AC power transmission over a cable rope

V M Rulevskiy[1], V G Bukreev[2], E B Shandarova[2], E O Kuleshova[2], S M Shandarov[3] and Yu Z Vasilyeva[2]

[1] Research Institute of Automation and Electromechanics, Tomsk State University of Control Systems and Radioelectronics, 53, Belinsky Str., Tomsk, 634034, Russia
[2] Tomsk Polytechnic University, 30, Lenina Ave., Tomsk, 634050, Russia
[3] Tomsk State University of Control Systems and Radioelectronics, 40, Lenina Ave., Tomsk, 634050, Russia

E-mail: bukreev@tpu.ru, shandarovaelena@mail.ru, kuleshova@tpu.ru

Abstract. A modeling problem of the power system, which provides an AC power transmission to a submersible device over the conducting rope, was considered. The power supply system units and their parameters are described. The system multi-dimensional mathematical model in the variables state space with regard to the nonlinear characteristic of system elements is proposed.

1. Introduction

A power supply system (PSS) of an autonomous object with the power transmission over a cablerope should be improved. For this purpose, it is possible to apply the optimal controllers for efficient stabilization of voltage at consuming loads and minimization of weight and size characteristics for parametric and external disturbances [1-4]. Creating these regulators assumes the use of synthesis methods of complex objects modern control theory based on the description of dynamic processes in the variables state space [5, 6]. It should be noted that the system of differential equations in the Cauchy form is the most adequate mathematical model in the variables state space of many objects. It reflects the 'physics' of occurring phenomena and processes under certain assumptions. The number of differential equations must fully reflect elements properties of the power supply system representing an equivalent circuit with lumped parameters.

Figure 1 shows the structure of the PSS model, which provides an AC power transmission to a submersible device over the cable rope.

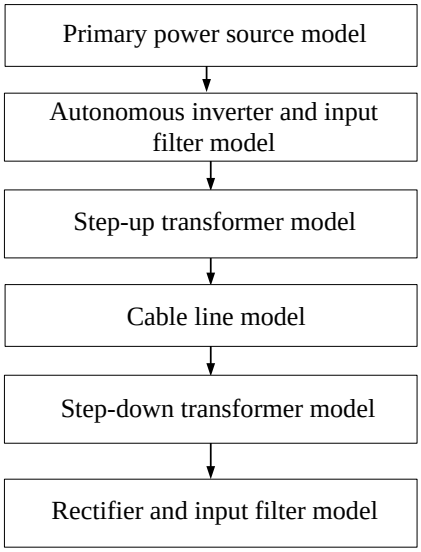

Figure 1. The structure of the PSS model.

It is assumed that parameters of the PSS equivalent circuit, shown in Figure 2, are the same for each phase in preparing mathematical models. It means that the system is symmetrical, and calculation can be carried out on one phase; other phases currents and voltages can be obtained by rotating through an angle of 120˚.

The power supply is an autonomous synchronous generator, and the rectifier connected through the output to an *L*-shaped *LC*-filter. The power supply model is not considered in this paper.

Supply voltage U_s (Figure 2) is assumed to be constant and devoid of pulsations as a result of a smoothing filter action in the preparation of the PSS mathematical model.

An independent voltage inverter (IVI) is a static inverter of DC voltage U_s to AC voltage via semiconductor switches, which are used as metal–oxide–semiconductor field-effect transistors (MOSFET-transistors). A power converter is controlled by the method of Pulse Width Modulation (PWM). An output voltage curve is formed as a series of high frequency pulses, the duration of which changes under the law of the modulating signal; clock frequency f_{ref} is equal to 48 kHz, and the modulation frequency – 1 kHz.

2. The mathematical model

The mathematical model made for the idealized inverter, assuming supply voltage U_s is constant and keys — ideal. Control pulses, supplied to the power transistor base, are formed as a result of comparing a modulated low-frequency three-phase voltage, having in its part the first and the third harmonic of the following form:

$$u_{Amd}(t)=\frac{\sin(1000t)+0.14\cdot\sin(3000t)}{\cos(30^\circ)};\ u_{Bmd}(t)=\frac{\sin(1000t-120^\circ)+0.14\cdot\sin(3000t)}{\cos(30^\circ)}$$

$$u_{Cmd}(t)=\frac{\sin(1000t+120^\circ)+0.14\cdot\sin(3000t)}{\cos(30^\circ)}$$

with the reference voltage of a sawtooth shape, shown in the model as Fourier series:

$$u_{ref}(t)=\frac{2}{\pi}\cdot\left(\sin(\omega_{ref}t)-\frac{1}{2}\sin(2\omega_{ref}t)+\frac{1}{3}\sin(3\omega_{ref}t)-\frac{1}{4}\sin(4\omega_{ref}t)+\ldots\right),$$

where $\omega_{ref}=2\pi f_{ref}$ is an angular clock frequency.

Application of the third harmonic premodulation increases the maximum achievable ratio of the first harmonic amplitude to power supply voltage U_s and then leads to a marked reduction in harmonic

distortion.

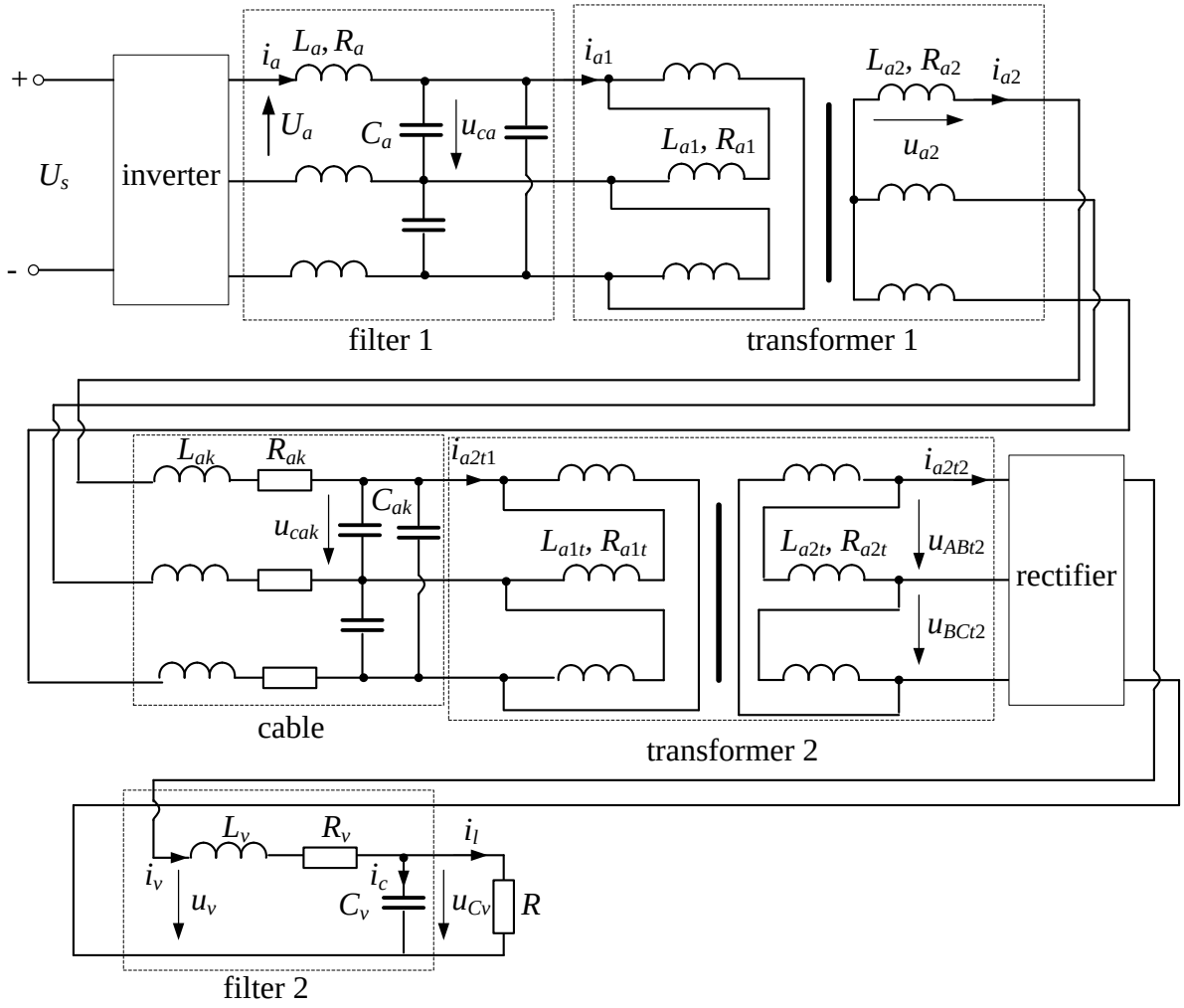

Figure 2. The PSS equivalent circuit.

The difference function is calculated for each phase according to the following formulas:

$$f_{Adif}(t) = u_{Amd}(t) - u_{ref}(t);\ f_{Bdif}(t) = u_{Bmd}(t) - u_{ref}(t);\ f_{Cdif}(t) = u_{Cmd}(t) - u_{ref}(t).$$

The phase switching function is recorded on the basis of the abovementioned formulas:

$$K_A(t) = \begin{Bmatrix} 1 \text{ if } f_{Adif} \geq 0 \\ 0 \text{ if } f_{Adif} < 0 \end{Bmatrix};\ K_B(t) = \begin{Bmatrix} 1 \text{ if } f_{Bdif} \geq 0 \\ 0 \text{ if } f_{Bdif} < 0 \end{Bmatrix};\ K_C(t) = \begin{Bmatrix} 1 \text{ if } f_{Cdif} \geq 0 \\ 0 \text{ if } f_{Cdif} < 0 \end{Bmatrix}.$$

The total commutation function autonomous inverter is written as:

$$K(t)=\left\{\begin{array}{l}-1/6 \text{ if } K_A(t)=1 \wedge K_B(t)=-1 \wedge K_C(t)=1\\ 1/6 \text{ if } K_A(t)=1 \wedge K_B(t)=-1 \wedge K_C(t)=-1\\ -1/6 \text{ if } K_A(t)=1 \wedge K_B(t)=1 \wedge K_C(t)=-1\\ 1/6 \text{ if } K_A(t)=-1 \wedge K_B(t)=1 \wedge K_C(t)=-1\\ -1/6 \text{ if } K_A(t)=-1 \wedge K_B(t)=1 \wedge K_C(t)=1\\ 1/6 \text{ if } K_A(t)=-1 \wedge K_B(t)=-1 \wedge K_C(t)=1\\ 1/2 \text{ if } K_A(t)=-1 \wedge K_B(t)=-1 \wedge K_C(t)=-1\\ -1/2 \text{ if } K_A(t)=1 \wedge K_B(t)=1 \wedge K_C(t)=1\end{array}\right\}$$

The mathematical model of the *L*-shaped output filter (Figure 2) for phase *A* can be written using such obtained switching function as:

$$\frac{di_a(t)}{dt}=\frac{-R_a}{L_a}\cdot i_a(t)+\frac{-1}{L_a}\cdot u_{Caz}(t)+\left(\frac{K_A(t)}{2L_a}+\frac{K(t)}{L_a}\right)\cdot U_s;\ \frac{du_{Caz}(t)}{dt}=\frac{1}{C_{az}}\cdot i_a(t),$$

where R_a [Ohm], L_a [mH], C_{az} [uF] (capacities have a star connection) – are parameters of the IVI output filter, which is shown as filter 1 in Figure 2, $u_{Caz}(t)$ - is a voltage across capacities, at the star connection.

The basis of the three-phase step-up and step-down transformer model in Figure 2 is a T-equivalent circuit [7, 9].

The transformers parameters are windings active resistance (R_{a1}, R_{a2}, R_{a1t}, R_{a2t}) and leakage inductance (L_{a1}, L_{a2}, L_{a1t}, L_{a2t}), taking into account the leakage flux influence. A transfer characteristic is modeled by the branch, containing active magnetic resistance R_{m1} for the first transformer and R_{m2} — for the second one (it simulates active losses in the core), and, respectively, L_{m1} and inductance L_{m2} (it simulates reactive core loss). The core saturation can be taken into account via the transfer characteristic, which is described by a piecewise linear approximation of the relation between the flux and magnetizing current (hysteresis was not considered). A saturation can also be considered as an introduction of saturated parameters to the model in the static modes simulation.

It should be noted that the special transformers were designed to operate in the considered power supply system.

Active-inductive load with the star-connection and parameters R_{eqv} [Ohms], L_{eqv} [mH] was connected to the secondary winding of the step-down transformer for recording the mathematical model. As it is seen from Figure 2 the step-down transformer is a transformer 2. Load parameters are calculated as the equivalent for the second filter and load at its output according to the known methods: if the parameters of the filter and load are known, the circuit complex resistance is calculated at the rectifier fundamental frequency. Active and reactive components of the complex resistance parameters allow calculating an equivalent load [8].

Cable line design features must be taken into account when designing their models. Cable line main parameters are: phase active resistance, distributed internal inductance of phases, phase distributed capacity relative to the screen, and the interphase mutual inductance and capacitance. In general case, the listed parameters are different for each plot. It is due to variation of manufacturing parameters, insulation depreciation, different qualities of the electrical connections in couplings [9]. Besides, the cable parameters are different in various areas due to the wide range of ambient temperature change depending on the depth of submersible device suspension.

Conduction currents were not taken into account when simulating the mathematical model of the cable line, because the value of the active conduction current through the cable insulation was less than 0.01%, and the value of the capacitive conduction current — less than 0.4% of the cable rated current [10].

A cable line can be simulated as a line with distributed and lumped parameters. The model with

lumped parameters, which is shown in Figure 2 as «cable» unit, was chosen as the mathematical model because of its simplicity and clarity.

The three-phase bridge rectifier, which is represented in Figure 2 as « rectifier» unit, is shown in the transfer function model, where rectified voltage U_v at intervals equaling to one-sixth of the period defined by difference-phase transformer EMF $u_{ABt2}, u_{BCt2}, u_{CAt2}$:

$$u_v = \begin{Bmatrix} u_{ABt2} - u_{BCt2} \text{ if } u_{ABt2} > u_{BCt2} \ \wedge \ u_{ABt2} \geq u_{CAt2} \wedge \ u_{BCt2} < u_{ABt2} \wedge \ u_{BCt2} \leq u_{CAt2} \\ u_{ABt2} - u_{CAt2} \text{ if } u_{ABt2} \geq u_{BCt2} \ \wedge \ u_{ABt2} > u_{CAt2} \wedge \ u_{CAt2} < u_{ABt2} \wedge \ u_{CAt2} \leq u_{BCt2} \\ u_{BCt2} - u_{CAt2} \text{ if } u_{BCt2} \geq u_{ABt2} \ \wedge \ u_{BCt2} > u_{CAt2} \wedge \ u_{CAt2} < u_{BCt2} \wedge \ u_{CAt2} \leq u_{ABt2} \\ u_{BCt2} - u_{ABt2} \text{ if } u_{BCt2} \geq u_{CAt2} \ \wedge \ u_{BCt2} > u_{ABt2} \wedge \ u_{ABt2} < u_{BCt2} \wedge \ u_{ABt2} \leq u_{CAt2} \\ u_{CAt2} - u_{BCt2} \text{ if } u_{CAt2} \geq u_{BCt2} \ \wedge \ u_{CAt2} > u_{ABt2} \wedge \ u_{ABt2} < u_{CAt2} \wedge \ u_{BCt2} \leq u_{CAt2} \\ u_{CAt2} - u_{ABt2} \text{ if } u_{CAt2} \geq u_{ABt2} \ \wedge \ u_{CAt2} > u_{BCt2} \wedge \ u_{ABt2} < u_{CAt2} \wedge \ u_{ABt2} \leq u_{BCt2} \end{Bmatrix}.$$

In the rectifier simulation, the following assumptions were taken: switching processes do not affect the shape of the output voltage and current; valves are ideal.

The PSS mathematical model was compiled for one phase (phase *A* was selected) to reduce the system order taking into account that the system is symmetrical. In this case, all parameters with a Δ-connection were transformed into a Y-connection (index *z* in the equations). The equation in an integro-differential form according to the Kirchhoff laws was made up for the scheme shown in Figure 2, where state variables are expressed, for drawing up a system of differential equations in the Cauchy form. Thus, state variables currents of the first and second filter (i_a, i_v), line currents of primary and secondary transformers windings ($i_{a1}, i_{a2}\ i_{a2t1}, i_{a2t2}$), and the voltage across the capacitive element $\left(u_{Caz}, u_{Cakz}\right)$ were selected.

As a result, the PSS mathematical model is written as follows in the state space:

$$\begin{aligned} \frac{di_a}{dt} &= a_{11} \cdot i_a + a_{12} \cdot u_{Caz} + a_{13} \cdot \left(\frac{K_A(t)}{2L_a} + \frac{K(t)}{L_a} \right) \cdot U_s; \\ \frac{di_{a1}}{dt} &= a_{21} \cdot i_{a1} + a_{22} \cdot i_{a2} + a_{23} \cdot u_{Caz} + a_{24} \cdot u_{Cakz}; \\ \frac{di_{a2}}{dt} &= a_{31} \cdot i_{a1} + a_{32} \cdot i_{a2} + a_{33} \cdot u_{Caz} + a_{34} \cdot u_{Cakz}; \\ \frac{di_{a2t1}}{dt} &= a_{41} \cdot i_{a2t1} + a_{42} \cdot i_{a2t2} + a_{43} \cdot u_{Cakz}; \\ \frac{di_{a2t2}}{dt} &= a_{51} \cdot i_{a2t1} + a_{52} \cdot i_{a2t2} + a_{53} \cdot u_{Cakz}; \\ \frac{du_{Caz}}{dt} &= \frac{1}{C_{az}} \cdot i_a - \frac{1}{C_{az}} \cdot i_{a1}; \\ \frac{du_{Cakz}}{dt} &= \frac{1}{C_{akz}} \cdot i_{a2} - \frac{1}{C_{akz}} \cdot i_{a2t1}, \end{aligned} \qquad (1)$$

where $L_{\Sigma 1} = L_{a1z}\left(L_{m1}k_1^2 + L_{a2} + L_{ak}\right) + L_{m1}\left(L_{a2} + L_{ak}\right)$; $L_{\Sigma 2} = L_{m2}\left(L_{a1tz}k_2^2 + L_2\right) + L_2 L_{a1tz}$;

$k_1, k_2 -$ the ratio of the secondary winding phase voltage to the primary winding phase voltage for the first and second transformers, respectively;

$R_2 = R_{a2tz} + R_{eqv}$; $L_2 = L_{a2tz} + L_{eqv}$;

$$a_{11}=-\frac{R_a}{L_a};\quad a_{12}=-\frac{1}{L_a};\ a_{13}=-\frac{1}{L_a};\ a_{21}=\frac{-L_{a2}\left(R_{m1}+R_{a1z}\right)-L_{ak}\left(R_{m1}+R_{a1z}\right)-L_{m1}k_1^2R_{a1z}}{L_{\Sigma1}};$$

$$a_{22}=\frac{-L_{m1}k_1\left(R_{a2}+R_{ak}\right)+k_1R_{m1}\left(L_{a2}+L_{ak}\right)}{L_{\Sigma1}};\ a_{23}=\frac{L_{a2}+L_{ak}+L_{m1}k_1^2}{L_{\Sigma1}};\ a_{24}=\frac{-L_{m1}k_1}{L_{\Sigma1}};$$

$$a_{31}=\frac{k_1\left(R_{m1}L_{a1z}-L_{m1}R_{a1z}\right)}{L_{\Sigma1}};\quad a_{32}=\frac{-L_{m1}\left(R_{a2}+R_{ak}\right)-L_{a1z}\left(R_{a2}+R_{ak}+R_{m1}k_1^2\right)}{L_{\Sigma1}};$$

$$a_{33}=\frac{L_{m1}k_1}{L_{\Sigma1}};\ a_{34}=\frac{-L_{a1z}-L_{m1}}{L_{\Sigma1}};\ a_{41}=\frac{-L_2\left(R_{m2}+R_{a1tz}\right)-L_{m2}k_2^2R_{a1tz}}{L_{\Sigma2}};\quad a_{42}=\frac{k_2\left(R_{m2}L_2-L_{m2}R_2\right)}{L_{\Sigma2}};$$

$$a_{43}=\frac{L_2+L_{m2}k_2^2}{L_{\Sigma2}};\ a_{51}=\frac{k_2\left(R_{m2}L_{a1tz}-L_{m2}R_{a1tz}\right)}{L_{\Sigma2}};\quad a_{52}=\frac{L_{a1tz}\left(-R_{m2}k_2^2-R_2\right)-L_{m2}R_2}{L_{\Sigma2}};\ a_{53}=\frac{L_{m2}k_2^2}{L_{\Sigma2}}.$$

The phase voltage at the first and second transformer output is calculated through the state variables:

$$u_{a2}=b_{11}\cdot i_{a1}+b_{12}\cdot i_{a2}+b_{13}\cdot u_{Caz}+b_{14}\cdot u_{Cakz};\quad u_{At2}=b_{21}\cdot i_{a2t1}+b_{22}\cdot i_{a2t2}+b_{23}\cdot u_{Cakz},$$

where

$$b_{11}=\frac{L_{ak}k_1\left(R_{m1}L_{a1z}-L_{m1}R_{a1z}\right)}{L_{\Sigma1}};$$

$$b_{12}=\frac{L_{m1}\left(L_{a2}R_{ak}-L_{ak}R_{a2}+R_{ak}k_1^2L_{a1z}\right)+L_{a1z}\left(L_{a2}R_{ak}-L_{ak}R_{a2}-L_{ak}k_1^2R_{m1}\right)}{L_{\Sigma1}};$$

$$b_{13}=\frac{L_{m1}k_1L_{ak}}{L_{\Sigma1}};\ b_{14}=\frac{L_{a2}\left(L_{m1}+L_{a1z}\right)+L_{m1}k_1^2L_{a1z}}{L_{\Sigma1}};\quad b_{21}=\frac{L_vk_2\left(R_{m2}L_{a1tz}-L_{m2}R_{a1tz}\right)}{L_{\Sigma2}};$$

$$b_{22}=\frac{L_{m2}\left(L_2R_v-L_vR_2\right)+L_{a1tz}\left(L_2R_v-L_vR_2+k_2^2\left(L_{m2}R_v-L_vR_{m2}\right)\right)}{L_{\Sigma2}};\ b_{23}=\frac{L_{m2}L_vk_2}{L_{\Sigma2}}.$$

The voltage and the current of the rectifier load, which is shown in Figure 2, are calculated according to formulas:

$$\frac{di_v}{dt}=\frac{R_v}{L_v}\cdot i_v+\frac{1}{L_v}\cdot u_v+\frac{1}{L_v}\cdot u_{Cv};\quad \frac{du_{Cv}}{dt}=\frac{1}{C_v}\cdot i_C,\tag{2}$$

where $i_C=i_v-\frac{1}{R}\cdot u_{Cv}$ and $i_l=\frac{1}{R}\cdot u_{Cv}$.

As a result, the mathematical model of PSS in the space of state variables is described as the system of equations (1) and (2).

3. Conclusion

The mathematical model for the power supply system of an autonomous object with an AC power transmission over a cable rope is described in the paper. The differential equations, describing a symmetrical three-phase power supply system, are presented in the Cauchy form. Thus, the model was developed, which allows determining the currents of input and output filters, linear currents of the primary and secondary transformer windings, the output voltage of the rectifier. The mathematical model simulation was carried out in MathCAD software tools. The advantage of this model is the ability to obtain values of the abovementioned voltages and currents, both in a steady state and during transients. Thus, this model allows one to reset and release a load current.

References

[1] Xiang X, Niu Z, Lapierre L and Zuo M 2015 *Hong Kong Institution of Engineers* **22** 103-116
[2] Song B, Zhang B, Jiang J 2016 *J. of Huazhong Univ. of Science and Techn.* **44** (7) 52-56
[3] Maalouf D, Creuze V, Chemori A, Tamanaja I T, Mercado E C, Muñoz J T, Lozano, R, Tempier O 2015 *Int. J. of Adv. Robotic Systems* **12** 1-15
[4] Cui R, Zhang X and Cui D 2016 *Ocean Engineering* **123** 45-54
[5] Fang M-C, Hou C-S and Luo J-H 2007 *Ocean Engineering* **34** (8-9) 1275-89
[6] Shilin A A. and Bukreev V G 2014 *Thermal Eng.* **61** (10) 741-746
[7] Vasileva O V, Budko A A and Lavrinovich A V 2016 *IOP Conf. Ser.: Mater. Sci. Eng*. (Tomsk) vol 124 (Bristol: IOP Publishing Ltd.) 012107
[8] Koran A, Labella T, Lai J-S 2014 *IEEE Transact. on Power Electr.* **29** 1285-1297
[9] Bychkov P N, Zabrodina I K, Shlapak V S 2016 *IEEE Transact. on Dielectrics and Electr. Ins.* **23** 288-293
[10] Kuleshova E O, Plyusnin A A, Shandarova E B, Tikhomirova O V 2016 *IOP Conf. Ser.: Mater. Sci. Eng.* (Tomsk) vol 124 (Bristol: IOP Publishing Ltd.) 012069